OIPE — APR 0 8 2005 — PATENT & TRADEMARK OFFICE — JC37

IN THE UNITED STATES PATENT AND TRADEMARK OFFICE

Applicant	:	Mark F. McCarty
Appl. No.	:	09/912,472
Filed	:	July 24, 2001
For	:	CHROMIUM/BIOTIN TREATEMNT OF TYPE II DIABETES
Examiner	:	Rebecca Cook
Group Art Unit	:	1614

BEST AVAILABLE COPY

FIRST DECLARATION OF JAMES KOMOROWSKI UNDER 37 C.F.R. § 1.132

Assistant Commissioner for Patents
Washington, D.C. 20231

Dear Sir:

I, James Komorowski, declare and state as follows:

1.   I am the Vice President of Technical Services & Scientific Affairs at Nutrition 21, Inc. ("Nutrition21"), the assignee of the above-captioned patent application. A significant portion of our research at Nutrition 21 targets the diabetes marketplace.

2.   I received a Bachelor of Arts degree in biology from State University of New York and a M.S. in medical biology from Long Island University.

3.   I have extensive experience in the field of diabetes-related research. I joined Nutrition 21 in 1997. From 1997-1999 I served as Senior Manager of Clinical and Regulatory Affairs. In 1999, I became Director of Product Development, and 2001 moved to my current position as Vice President of Technical Services and Scientific Affairs at Nutrition 21. Prior to my employ at Nutrition 21, I spent nine years in the pharmaceutical industry, holding product management, clinical research, and regulatory affairs positions at major pharmaceutical companies. Additionally, I have worked for a number of years in academia as a research associate at both New York Hospital for Special Surgery and Memorial Sloan-Kettering Cancer Center

4.   As one who has had familiarity with in the field of diabetes research for several years, I am intimately familiar with the underlying causes of this disease, as well as the symptoms and risk factors associated therewith. The hallmark of diabetes is increased blood glucose levels, or
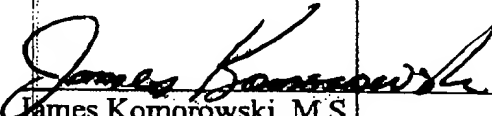
?

hyperglycemia. Various underlying causes of hyperglycemia and diabetes in individuals exist. For example, it is well known that Type I Diabetes arises from an absolute deficiency in insulin secretion by pancreatic cells. Type II Diabetes arises from a combination of defects in insulin secretion and defects in cells' abilities to respond to insulin (i.e., insulin resistance). Although there is variation in the underlying cause of diabetes, since the end result is hyperglycemia, diabetes therapy is typically aimed at ameliorating this condition. In fact, the most important factor in treating Type II Diabetes is the treatment of hyperglycemia.

5.   This principle is shown in the Position Statement authored by the American Diabetes Association entitled "Diagnosis and Classification of Diabetes Mellitus," ((2005), *Diabetes Care*, Vol 28, Supp. 1, S37-S42), and in the portion of the Center for Disease Control's website regarding frequently asked questions about diabetes. (http://www.cdc.gov/diabetes/faq/basics.htm, last visited 3/15/05). The American Diabetes Association, which is a leading organization in the field of diabetes, defines diabetes as a group metabolic diseases characterized by hyperglycemia. The Position Statement describes the known underlying causes of hyperglycemia, as well as diabetes treatments aimed at treating this condition. The Center for Disease Control, a leading research institution with vast expertise in the field of diabetes, also defines diabetes as "a disease in which blood glucose levels are above normal," and discusses the maintenance of glucose levels within an acceptable range as the "treatment for diabetes."

6.   I hereby declare that all statements made herein of my own knowledge are true and that all statements made on information or belief are believed to be true, and further that these statements were made with the knowledge that willful false statements and the like so made are punishable by fine or imprisonment, or both, under Section 1001 of Title 18 of the United States Code and that such willful statements may jeopardize the validity of the application of any patent issued thereon.

Date: _~April 5, 2005~_____   _~James Komorowski~_____

                                        James Komorowski, M.S.

1434276_1
032305

IN THE UNITED STATES PATENT AND TRADEMARK OFFICE

Applicant	:	Mark F. McCarty
Appl. No.	:	09/912,472
Filed	:	July 24, 2001
For	:	CHROMIUM/BIOTIN TREATEMNT OF TYPE II DIABETES
Examiner	:	Rebecca Cook
Group Art Unit	:	1614

SECOND DECLARATION OF JAMES KOMOROWSKI, UNDER 37 CFR §1.132

Commissioner for Patents
P.O. Box 1450
Alexandria, VA 22313-1450

Dear Sir:

I, James Komorowski, declare and state as follows:

1. I am the Vice President of Technical Services & Scientific Affairs at Nutrition 21, Inc. ("Nutrition21"), the assignee of the above-captioned patent application. Our research at Nutrition 21 targets the diabetes marketplace.

2. I received a Bachelor of Arts degree in biology from State University of New York and a M.S. in medical biology from Long Island University.

3. I have extensive experience in investigating the role of chromium and other nutrients in ameliorating metabolic disorders, including, among others, hyperglycemia. I joined Nutrition 21 in 1997. From 1997-1999, I served as Senior Manager of Clinical and Regulatory Affairs. In 1999, I became Director of Product Development, and 2001 moved to my current position as Vice President of Technical Services and Scientific Affairs at Nutrition 21. Prior to my employ at Nutrition 21, I spent nine years in the pharmaceutical industry, holding product management, clinical research, and regulatory affairs positions at major pharmaceutical companies. Additionally, I have worked for a number of years in academia as a research associate at both New York Hospital for Special Surgery and Memorial Sloan-Kettering Cancer Center.

4.   Throughout the course of my career, I have completed more than 100 research studies, submitted over 10 regulatory submissions to the FDA, and am an inventor on over 12 patents. I lead Nutrition 21's scientific research team.

5.   Since I joined Nutrition 21, I have been involved in the design and implementation of studies to assess the effects of selected nutrients on glucose uptake in humans. To this end, I oversaw the development and adaptation of a model system using human skeletal muscle cultures to screen candidate nutrients for beneficial effects in the regulation of carbohydrate metabolism in humans. The usefulness of this system as a model for glucose metabolism in non-insulin dependent diabetes mellitus is set forth in Henry et al. ((1995), *Diabetes*, 44:936-946), attached hereto as Exhibit A.

6.   Based on their postulated role in carbohydrate metabolism, biotin, picolinic acid, arginine, α-lipoic acid, N-actylcysteine, Reservatol, and Conjugated Linoleic Acid were tested alone or in combination with chromium picolinate (CrPic) for their ability to affect insulin-mediated glucose uptake in skeletal muscle cultures, as a model for the metabolic disorder that characterizes Type II Diabetes. Prior to the *in vitro* experiments measuring glucose uptake, it was not known whether the nutrients tested would have any effect, an additive effect, or a synergistic effect, on insulin mediated glucose uptake in the presence of CrPic.

7.   To assess glucose uptake, [³H]C-deoxyglucose was added to cultures of skeletal muscle, in media with or without insulin and the test nutrients, and uptake of the labeled glucose by the cells was calculated.

8.   The results from these experiments are presented in Table 2, which forms part of this Declaration (Exhibit B). The first column in Table 2 identifies the nutrient tested. The second column ("Concentration") indicates concentration of the test nutrient(s) added to the culture media. The "Control" row refers to cultures in which no nutrients or CrPic was added, and reflects the baseline level of insulin-mediated glucose uptake in the absence of any nutrients. The ability to affect insulin-mediated glucose uptake is measured in the "Glucose Uptake" columns, and is reported in terms of "% change," in the final column.

9.   The *in vitro* data generated with the skeletal muscle model system revealed the unexpected result that the combination of CrPic with Biotin enhanced glucose uptake when compared to the stimulation of glucose uptake seen with CrPic alone or Biotin alone (i.e., the combination exhibited a synergistic effect), as shown in Table 2. Of the nutrients tested, biotin was one of the nutrients tested that worked synergistically with chromium picolinate to enhance glucose uptake. A graphical depiction of the synergistic effect is shown in the Figure entitled "Glucose Uptake in Human Skeletal Muscle Cells," attached hereto as Exhibit C. Exhibit C indicates that chromium picolinate alone caused a 0.16 change in glucose uptake levels. Biotin alone had almost no effect on glucose uptake levels. The combination of biotin and chromium picolinate, however showed a dramatic 0.65 change in glucose uptake levels.

10.   I hereby declare that all statements made herein of my own knowledge are true and that all statements made on information or belief are believed to be true, and further that these statements were made with the knowledge that willful false statements and the like so made are punishable by fine or imprisonment, or both, under Section 1001 of Title 18 of the United

Appl. No.   :   09/912,472
Filed   :   July 24, 2001

States Code and that such willful statements may jeopardize the validity of the application or any patent issued thereon.

By: _James Komorowski_   Date:_April 5, 2005_
     James Komorowski

1433331_2
032305

Insulin Action and Glucose Metabolism in Nondiabetic Control and NIDDM Subjects

Comparison Using Human Skeletal Muscle Cell Cultures

Robert R. Henry, Leslie Abrams, Svetlana Nikoulina, and Theodore P. Ciaraldi

Myoblasts from human skeletal muscle were isolated from needle biopsy samples of vastus lateralis and fused to differentiated multinucleated myotubes. Specific high-affinity insulin and insulin-like growth factor I (IGF-I) binding, glucose transporter proteins GLUT1 and GLUT4, glycogen synthase and pyruvate dehydrogenase proteins, and their specific mRNAs were identified in fused myotubes. Insulin and IGF-I stimulated 2-deoxyglucose uptake twofold with half-maximal stimulation by insulin at 0.98 ± 0.12 nmol/l and maximal stimulation at 17.5 nmol/l. Acute insulin treatment (33 nmol/l) doubled glycogen synthase activity and glucose incorporation into glycogen while increasing pyruvate dehydrogenase ~30%. In cells cultured from NIDDM subjects, both basal (6.9 ± 1.0 vs. 13.0 ± 1.7 pmol $\cdot$ mg protein$^{-1} \cdot$ min^{-1}) and acute insulin-stimulated transport (13.5 ± 2.0 vs. 22.4 ± 1.3 pmol $\cdot$ mg protein$^{-1} \cdot$ min^{-1}) were significantly reduced compared with nondiabetic control subjects (both $P \leq 0.005$). GLUT1 protein content of total membranes from NIDDM subjects was decreased compared with control subjects, while GLUT4 levels were similar between groups. A significant correlation ($r = 0.65, P \leq 0.05$) was present when maximal rates of insulin-stimulated glucose transport in cell culture from subjects were compared with their corresponding in vivo glucose disposal determined by hyperinsulinemic glucose clamp. In summary, differentiated human skeletal muscle cultures exhibit biochemical and molecular features of insulin-stimulated glucose transport and intracellular enzyme activity comparable with the in vivo situation. Defective insulin-stimulated glucose transport persists in muscle cultures from NIDDM subjects and resembles the reduced insulin-mediated glucose uptake present in vivo. We conclude that this technique provides a relevant cellular model to study insulin action and glucose metabolism in normal subjects and determine the mechanisms of insulin resistance in NIDDM. *Diabetes* 44:936–946, 1995

Skeletal muscle is the principal site of insulin-mediated glucose uptake and utilization in humans (1), and several disorders including obesity and NIDDM are characterized by impaired insulin action in this tissue (2,3). Investigations into the mechanisms of insulin action and carbohydrate metabolism in both normal and insulin-resistant states have been hampered, however, by difficulties in accurately assessing both in vivo and in vitro events in this primary target tissue. Interpretation of clinical studies are usually complicated by the inability to accurately localize events in this tissue due to the presence of multiple metabolic variables that cannot be adequately controlled or accounted for. Although in vitro assessment is less influenced by such confounding variables, studies are commonly conducted in cell cultures of animal species, which may not be relevant or suitable as models of human muscle tissue. Isolated samples of human muscle obtained at surgery or by biopsy have also been used to assess muscle glucose metabolism but are restricted by the static nature of measurements and the inability for longitudinal evaluation after metabolic manipulations. Many of these limitations have been overcome by the recent description of a human skeletal muscle cell (HSMC) culture system (4,5) that is suitable for metabolic studies.

In this report, we have utilized and adapted the ability to culture human skeletal muscle to evaluate insulin action and glucose metabolism in normal and NIDDM subjects using small amounts of muscle obtained by needle biopsy of vastus lateralis. The preparation, growth, and characterization of these cultures is detailed and demonstrates that after fusion and differentiation, muscle cells manifest both basal and insulin-stimulated glucose transport as well as intracellular glucose metabolism that resembles the in vivo situation. We have also shown that cultured muscle cells from subjects with NIDDM continue to manifest defects of insulin-stimulated glucose transport, which may reflect the impaired muscle glucose uptake present in vivo.

RESEARCH DESIGN AND METHODS

Materials. All radioisotopes were obtained from Du Pont-NEN (Boston, MA). The fluorescent probes tetramethylrhodamine isothiocyanate (TRITC) and Hoechst dye 33342 were obtained from Molecular Probes (Eugene, OR). Muscle biopsy needles were purchased from Baxter V. Mueller (McGaw Park, IL). Biotinylated rabbit anti-mouse IgG was obtained from Vector (Burlingame, CA) and streptaviden-fluorescein isothiocyanate (FITC) from Zymed (San Francisco, CA). Monoclonal mouse anti-rabbit skeletal myosin fast (heavy-chain) antibody was

TABLE 1
Subject characteristics

	Normal subjects	NIDDM subjects
n	14	11
Age (years)	42 ± 2	50 ± 2*
Body mass index (kg/m^2)	27.5 ± 1.0	30.4 ± 1.2
Insulin (pmol/l)	36 ± 12	102 ± 3*
Fasting plasma glucose (mmol/l)	5.2 ± 0.1	8.8 ± 0.9*
Oral glucose tolerance test (2 h, 75 g)		
Glucose (mmol/l)	6.0 ± 0.1	14.9 ± 1.2*
Insulin (pmol/l)	382 ± 93	293 ± 71

Data are means ± SE. *$P \leq 0.05$.

purchased from Sigma (St. Louis, MO). Polyclonal antibodies raised to the COOH-terminal sequences of both glucose transporter GLUT1 (RaGLUTRANS) and GLUT4 (RaIRGT) isoforms were obtained from East Acres Biologicals (Southbridge, MA). Human insulin, insulin-like growth factor I (IGF-I), [^{125}I-Tyr A^{14}]-monoiodoinsulin and [^{125}I-Tyr A^{14}]-monoiodo-IGF-I were provided by Lilly (Indianapolis, IN). Culture growth media (SkGM Bullet Kit) was obtained from Clonetics (San Diego, CA). Fetal bovine serum (FBS) was purchased from Gemini (Calabasas, CA). α-Minimum essential medium (MEM), trypsin/EDTA, Fungibact, glutamine, Ham's F-10 media, and horse serum were purchased from Irvine Scientific (Santa Ana, CA). Creatine kinase (CK) was purchased from Boehringer Mannheim (Indianapolis, IN). Protein assay reagent was purchased from BioRad (Hercules, CA). PGem4Z-Amt7 (GLUT4) and pSGT (GLUT1) were acquired from the American Type Culture Collection (Rockville, MD). The Riboprobe Gemini system used to construct RNA probes was obtained from Promega (Madison, WI). Restriction enzymes and the random primer DNA labeling kit were purchased from BRL (Gaithersburg, MD). RNA STAT-60 was obtained from Tel-Test B (Friendswood, TX). Anti-rabbit IgG conjugated with horseradish peroxidase and the ECL chemiluminescence kit were obtained from Amersham (Arlington Heights, IL). XAR-5 film was obtained from Eastman-Kodak (Rochester, NY). All other reagents and chemicals were purchased from Sigma.

Human subjects. The clinical characteristics of nondiabetic and NIDDM subjects (6) who provided muscle tissue for these studies are summarized in (Table 1). All subjects studied were men. The experimental protocol was approved by the Committee on Human Investigation of the University of California, San Diego (UCSD). After explanation of the protocol, written informed consent was obtained from all subjects.

Glucose disposal rates. Of the 25 subjects who had needle muscle biopsies, 17 (13 nondiabetic and 4 NIDDM) also had in vivo rates of glucose disposal determined on a separate day using the hyperinsulinemic glucose clamp technique. Procedures of the clamp study have been described in detail previously (7). In brief, [3-^{3}H]glucose was infused in a continuous manner throughout the entire study, beginning at least 3 h before the infusion of insulin. Insulin was infused in a primed continuous manner at 720 pmol · m^{-2} · min^{-1}, and plasma glucose was held constant at 5.0–5.5 mmol/l for 4–5 h. The glucose disposal rate (in mg · kg^{-1} · min^{-1}) was calculated during the final 40 min of each clamp study from the isotopically determined rate of glucose disappearance (R_d) corrected for changes in plasma glucose within its distribution space.

Muscle biopsy technique. Percutaneous muscle biopsies were performed on the lateral portion of the quadriceps femoris (vastus lateralis) using a 5-mm diameter side-cutting needle as described in detail previously (7). Tissue (250–400 mg) was obtained and processed immediately as described below.

Skeletal muscle culture procedure. Growth of HSMCs was carried out using modifications of the methods of Blau and Webster (8) and Sarabia et al. (9). At the time of biopsy, muscle tissue was placed in 15 ml Ham's F-10 media at 4°C and carefully dissected, minced, and washed three times with F-10 media at 4°C and once at 37°C to aid in removal of connective tissue. The tissue was then dissociated by three successive treatments of 20 min each in 25 ml 0.05% trypsin/EDTA at room temperature. Dissociated cells were centrifuged at 600g for 4 min at 37°C and resuspended in fully supplemented human skeletal growth media (SkGM BulletKit) with 2% FBS and no added insulin. Cells were plated on 100-mm dishes and placed in an incubator containing 95%

air/5% CO_2; media were changed every 3–4 days until 70–80% confluence was obtained (4–6 weeks).

To distinguish and separate myoblasts from potential contamination with fibroblasts, immunofluorescent flow cytometry using 5.1H11, a monoclonal antibody that specifically recognizes a human muscle cell surface antigen (10) (provided by Dr. H. M. Blau, University of California, San Francisco), was used with a second antibody and fluorescent tag. For fluorescent sorting, cells were resuspended in F-10 media plus 1% horse serum and analyzed using a FACStar Plus with an argon-ion laser (Becton-Dickinson, Mountain View, CA).

Each needle biopsy procedure of 250–400 mg yielded ~1–2 × 10^6 myoblasts. Cell number was determined using a 1-mm counting chamber and a light microscope. For studies of glucose transport, cells were plated in 12-well tissue culture dishes at a density of 6,000 cells/well. Insulin and IGF-I binding were measured in 24-well plates seeded with 4,000 cells/well. For other studies, 15,000–20,000 cells were plated on 100-mm dishes. Growth was reestablished in specialized SkGM media without added insulin plus 2% FBS until 70–80% confluence was reached (average 3–4 weeks). At this stage, these first-pass cells were uniformly fused and differentiated into myotubes to prevent spontaneous fusion, resulting in variable mixtures of myoblasts and myotubes. Fusion was achieved after 4 days growth in α-MEM with 2% FBS and 1% penicillin (200 U/ml)/streptomycin (200 mg/ml). In a series of preliminary studies (data not shown), it was determined that the metabolic responsiveness of these cells was optimal after 4 days of fusion. Therefore, except where noted, all experiments were performed on 4-day fused myotubes of first-pass cells. Muscle differentiation into myotubes was determined from histological evidence of multinucleation from fluorescent microscopy, from induction of sarcomeric α-actin protein on Western blot and CK-M mRNA by slot blot analysis (all described below), and from CK enzyme activity (expressed as U/mg protein) determined by a spectrophotometric assay according to the manufacturer's instructions.

Structural analysis. To confirm fusion, cell cultures were fixed in 3.7% formaldehyde in phosphate-buffered saline (PBS) for 30 min at room temperature. Myoblasts and myotubes were stained with fluorescent probes using 5 mmol/l TRITC (11) to label protein and 10 mmol/l Hoechst dye 33342 (12) to label nuclear DNA. To visualize skeletal muscle striations, myotubes were permeabilized with 0.2% Triton X-100 in PBS for 15 min at room temperature, blocked with 10% normal goat serum, and incubated with primary antibody (monoclonal anti-α-sarcomeric actin) for 120 min (13). After being washed with PBS, cells were incubated with FITC-conjugated rabbit anti-mouse IgG secondary antibody and mounted in Gelvatol. Cells were observed using a fluorescence microscope (Olympus BH2-RFC, Tokyo, Japan) at an excitation wavelength of 546 nm from parallel cultures subsequently used for metabolic studies. Visual estimates of multinucleated myotubes were made from stained plates at the same time assays were performed.

Insulin and IGF-I receptor binding. To measure binding, cells were grown to near confluence in 24-well plates, followed by fusion and differentiation for 4 days. After washing four times with 0.5 ml room temperature reaction buffer of the composition (in mmol/l) 150 NaCl, 5 KCl, 1.2 MgSO$_4$, 1.2 CaCl$_2$, 2.5 NaH$_2$PO$_4$, 10 HEPES, and 1% bovine serum albumin, pH 7.6, 450 μl buffer was added to each well and incubated in triplicate with [^{125}I-Tyr A^{14}]insulin (final concentration 67 pmol/l) or [^{125}I-Tyr A^{14}]IGF-I (final concentration 39 pmol/l) at 24°C for 2 h in the absence and presence of varying concentrations of unlabeled hormone. The amount of receptor-bound hormone was determined after lysis with 1 N NaOH at 55°C on solubilized cell suspensions as described in detail previously (14).

2-Deoxyglucose transport. The procedure for glucose transport was a modification of the methods described by Klip et al. (15) for L6 myocytes. Cells were incubated with serum-free media containing varying concentrations of insulin (0–33 nmol/l) or IGF-I (0.66 and 26.4 nmol/l) for 60–90 min in a 95% O$_2$/5% CO$_2$ incubator at 37°C. Glucose uptake was determined in triplicate at each point after the addition of 10 μl substrate ([2-^{3}H]deoxyglucose/L-[^{14}C]glucose, 0.1 mCi, final concentration 0.01 mmol/l) to provide a concentration at which cell membrane transport is rate-limiting (16). The value for L-glucose uptake was subtracted to correct each sample for the contributions of diffusion and trapping. Protein content was determined on a 100-ml aliquot of the cell suspension using the Bradford method (17). Except when noted, glucose transport is expressed as pmol · mg protein^{-1} · min^{-1}.

Glycogen synthase (GS) and pyruvate dehydrogenase (PDH) enzyme activity. The activity of these enzymes was measured according to methods described in detail previously (18,19). In brief, fully fused myotube cultures were incubated at 37°C and 95% air/5% CO$_2$ in

serum-free α-MEM containing 5.5 mmol/l D-glucose for 1 h followed by 1 h treatment with or without 33 nmol/l insulin. After rinsing three times with 4°C PBS, GS buffer (18) was added to cultures, cells were scraped into Eppendorf tubes and sonicated (50 Sonic Dismembrator, Fisher, Tustin, CA) at setting 8 for 30 s at 4°C. GS activity was assayed at a physiological concentration of substrate (0.3 mmol/l UDP-glucose) and 0.1 and 10 mmol/l concentrations of the allosteric activator, glucose 6-phosphate. For PDH, cells were dislodged into 2 ml homogenization buffer (19) at 4°C and homogenized by 15 strokes of a Dounce homogenizer. After centrifugation at 20,000g for 20 min, the mitochondrial pellet was resuspended in 200 ml homogenization buffer and sonicated as above. PDH was determined in the presence of sodium fluoride to assay active PDH and in its absence to measure total PDH. Enzyme activities are expressed in nmol · mg protein^{-1} · min^{-1} and as fractional velocity (FV).

Glycogen synthesis. Glucose incorporation into glycogen was determined as described by Ciaraldi et al. (20). Fully fused myotubes were incubated at 37°C with 95% air/5% CO_2 for 1 h in serum-free α-MEM containing 5.5 mmol/l D-glucose. All studies were carried out in paired 100-mm dishes incubated as above for an additional 1 h in the presence or absence of 33 nmol/l insulin. D-[^{14}C-U]glucose (0.4 mCi/ml, 5 nl) was added with or without insulin to media of paired dishes for an additional hour, cells were lysed, and glycogen was collected. Results are expressed as nmol glucose converted to glycogen · mg protein^{-1} · h^{-1}.

Isolation and extraction of RNA. After growth in 100-mm dishes, total cellular RNA was extracted and purified by a single-step method using RNA STAT-60 according to the manufacturer's instructions.

Ribonuclease protection assay

Vector construction. Human muscle GS cDNA (21) (provided by Drs. Michelle Browner and Robert Fletterick, University of California, San Francisco) was digested with *Hind*III, and the fragment from nucleotides 414 to 1,367 was ligated into the Stratagene cloning vector BSSK. The plasmid was inserted into competent DH5 *Escherichia coli*. Based on the published human liver PDH E1α cDNA sequence (22), a 23-base oligonucleotide PDH primer was synthesized at the UCSD Peptide Synthesis Core Facility and annealed to total RNA isolated from human skeletal muscle. The antisense strand was synthesized beginning at nucleotide 906 of PDH using avian reverse transcriptase (23). Amplification of the fragment was carried out using the polymerase chain reaction (PCR). Oligonucleotide primers synthesized for this reaction included a 23-base 3' PDH primer with an internal *Pst* I site and a 30-base 5' PDH primer with an internal *Eco*RI site. These primers were used to amplify the PDH cDNA fragment from nucleotides 83 to 906 using the GeneAmp DNA amplification kit with AmpliTaq (24). The PCR product was digested with *Pst* I and *Eco*RI and electrophoresed on a 1% agarose gel with ethidium bromide. The band of interest was excised, and the DNA was eluted from the gel by dialysis. The PDH cDNA fragment was ligated into the Promega expression vector PGem 4Z and competent XL1-Blue *E. coli* were transformed with the resultant plasmid. For GLUT4 and GLUT1 probes, PGem 4Z-Amt7 was digested with *Xho* I, and the retrieved GLUT4 fragment from nucleotides 858 to 1,564 was ligated into PGem 4Z. pSGT was digested with *Pst* I and the retrieved GLUT1 fragment from nucleotides 75 to 600 ligated into PGem 4Z. Colonies for all inserts were initially screened by restriction fragment-length polymorphism and confirmed by sequence analysis using Sequenase (United States Biochemical, Cleveland, OH) T7 DNA polymerase (25). The Promega Riboprobe System was used to generate high specific activity, single-stranded RNA probes from the cloned DNA inserts according to the manufacturer's instructions. Full-length probes of 115, 139, 137, and 217 bases were generated for PDH, GS, GLUT1, and GLUT4, respectively.

Hybridization. A quantity of 25–115 µg of dried total RNA was hybridized to the purified probe after resuspension in 30 ml hybridization buffer (4 parts deionized formamide, 1 part 40 mmol/l PIPES, pH 6.4, 1 mmol/l EDTA, and 0.4 mol/l NaCl). The mixture was heated at 85°C for 3 min followed by incubation in a waterbath at 48°C overnight. Negative controls of probe plus yeast tRNA were prepared similarly.

Digestion. Each hybridization sample was mixed with 350 µl digestion buffer (10 mmol/l Tris HCl, pH 7.5, 300 mmol/l NaCl, 5 mmol/l EDTA, pH 8.0) containing 3 U RNase A and 0.5 U RNase T and incubated at 30°C for 1.5 h. After addition of 20 µl 10% sodium dodecyl sulfate (SDS) and 2.5 µl (20 mg/ml) of proteinase K, the sample was incubated for 15 min at 37°C, followed by phenol inactivation of proteinase K and chloroform-OH extraction. RNA-RNA hybrids were precipitated from the aqueous phase with ethanol, and the pellet was dried under vacuum. The pellet was resuspended in gel loading buffer, heated to 85°C for 3 min,

loaded onto a 6.5% polyacrylamide gel, and run at 400 V for 1.5 h using a vertical gel apparatus (JM Specialty Parts, San Diego, CA). The gel was fixed with 10% methanol/10% acetic acid for 15 min, dried, and exposed to XAR-5 film overnight. After development, bands were scanned and quantitated with a LKB Ultrascan XL densitometer (Uppsala, Sweden). Results are expressed as the ratio of the respective mRNA autoradiograph band intensity to β-actin signal per µg total RNA (see below).

Slot blots. DNA probes to rat skeletal muscle creatine phosphokinase (CPK-M) (provided by Dr. W. Dillman, UCSD) and the human β-actin gene (provided by Dr. J. Kusari, UCSD) were prepared using a BRL random primer DNA labeling kit according to manufacturer's protocol. Total RNA was applied to nitrocellulose (5 mg/slot) using a Minifold II slot blot apparatus (Schleicher and Schuell, Keene, NH) and the filter baked at 80°C for 2 h under vacuum. After washing, the filter was air-dried, exposed to XAR-5 film, and quantitated by scanning densitometry as described above. β-actin was measured to confirm that mRNA changes were specific and that equal amounts of total RNA were loaded on the filter.

Immunoblot analysis

Sample preparation. All samples for Western blotting were prepared from confluent monolayers of myoblasts or fused myotubes. For sarcomeric α-actin and GS protein, 700-µl aliquots of buffer (50 mmol/l HEPES, 10 mmol/l EDTA, 100 mmol/l NaF, 5 mmol/l dithiothreitol [DTT], 1 mmol/l leupeptin, 1 mmol/l pepstatin, 200 mmol/l phenylmethylsulfonyl fluoride [PMSF], pH 7.5) were added to each plate, the cells scraped with a rubber policeman into Eppendorf tubes and sonicated as for GS enzyme assay (18). For PDH, cells were prepared as described previously for determination of enzyme activity and mixed with 0.3 ml homogenization buffer at 4°C containing 2 mmol/l DTT, 50 mmol/l HEPES, 2 mmol/l EDTA, 2 mmol/l EGTA, 200 mmol/l PMSF, 1 mmol/l leupeptin, 1 mmol/l pepstatin, and 50 mmol/l NaF at pH 7.4 and homogenized by 15 strokes of a Dounce homogenizer. After centrifugation at 600g for 20 min, the mitochondrial pellet was resuspended in 200 µl buffer and sonicated as described above.

To detect glucose transporter protein, total membranes were prepared by a modification of the method developed by Klip and colleagues (4,26) for L6 and cultured human skeletal muscle cells. Cells were dislodged with a rubber scraper into 3 ml 4°C homogenization buffer containing 250 mmol/l sucrose, 5 mmol/l NaN_3, 2 mmol/l EGTA, 200 mmol/l PMSF, 1 mmol/l leupeptin, 1 mmol/l pepstatin, 20 mmol/l HEPES at pH 7.4. After centrifugation at 600g for 10 min, cells were homogenized by 20 strokes with a Dounce homogenizer. To remove nuclei and mitochondria, the homogenate was centrifuged at 750g for 3 min, the pellet rehomogenized and centrifuged as described above, and the supernatant was recentrifuged at 190,000g for 60 min to obtain the total membrane pellet. These membranes were resuspended in homogenization buffer, protein content determined, and stored at −70°C until analyzed. For immunoblotting, sources for commercial antibodies were listed under METHODS. In addition, anti-peptide antibodies raised to the COOH-terminus of both PDH E1α subunit (from Dr. B.J. Song at the National Institutes of Health in Bethesda, MD) and human muscle GS (from Dr. L. Groop in Malmo, Sweden) were also used.

Detection of cellular proteins. Sonicated samples for sarcomeric α-actin, GS, and PDH were solubilized in Laemmli's buffer with 5% β-mercaptoethanol while membrane preparations for GT proteins were diluted in Laemmli's buffer without β-mercaptoethanol (27). All samples were heated for 5 min at 90°C. Proteins were separated electrophoretically on 8% SDS–polyacrylamide gel electrophoresis (PAGE) gels for sarcomeric α-actin and GS, 10% gels for GLUT1 and 4 and 12% gels for PDH and then transferred to nitrocellulose (28). After blocking, transferred proteins were blotted with specific mono- or polyclonal antibodies, washed, and incubated with anti-rabbit or anti-mouse IgG conjugated with horseradish peroxidase. Immune complexes were detected using an enhanced chemiluminescence kit and quantified using a scanning densitometer.

Statistical analysis. Data calculations and statistical analysis were performed using the StatView program (Abacus Concepts, Berkeley, CA). All data are expressed as means ± SE. Statistical significance was tested with repeated measures analysis of variance followed by the Student's *t* test. Correlation coefficients were calculated using the method of least squares.

RESULTS

Cell culture structure and morphology. Initial analysis of fluorescently activated and sorted muscle cells confirmed
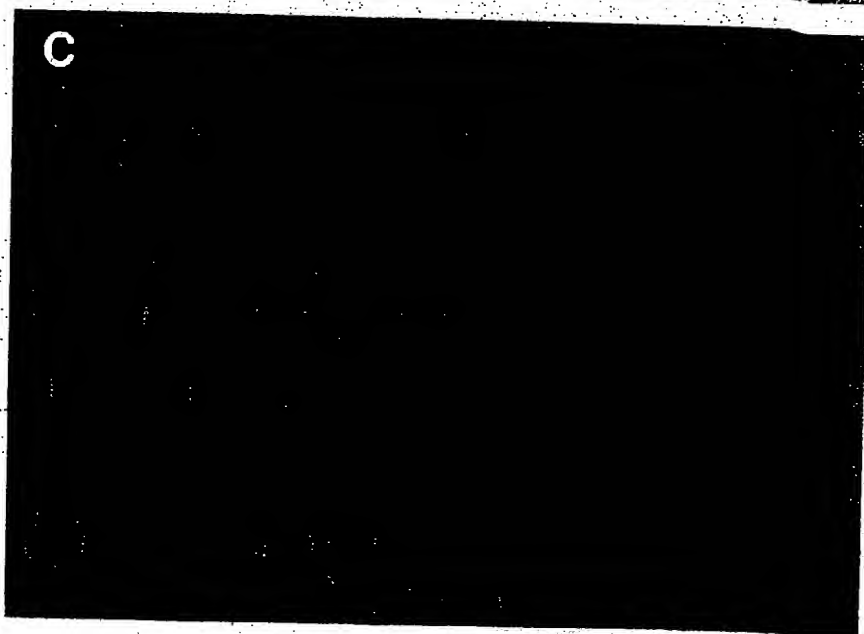
FIG. 1. Fluorescent micrographs of nonfused myoblasts (A), fused multinucleated myotubes (B), and fused myotubes stained for skeletal muscle-specific myosin-fast heavy chain (C) in HSMC cultures. Cells were formaldehyde-fixed and stained with fluorescent probes TRITC and Huechst 33342 dye (A and B) and monoclonal anti-myosin fast with FITC-conjugated rabbit anti-mouse IgG to demonstrate muscle striations (C). Micrographs are shown at ×60–120.

TABLE 2
Markers of HSMC differentiation

	Myoblasts (nonfused)	Myotubes (fused)
α-Actin (U/μg protein)	0.953	3,492
CPK activity (U/mg protein)	0.335 ± 0.095	2.068 ± 0.112*
CPK-M mRNA (arbitary units)	0.176 ± 0.028	0.351 ± 0.054*

Data are means ± SE. Arbitrary units are defined as the densitometric area of CPK mRNA per μg total RNA/β-actin mRNA per μg total RNA. CPK results are from cultures of five subjects. *$P \leq 0.01$.

that cultures were established from cells of pure (>99%) muscle (myoblast) origin (not shown). Since initial cell cultures were found to be consistently ≥90% myoblasts before cell sorting, fluorescent cell sorting was discontinued after the first 15 cultures. In this situation, growth was established and continued without sorting until cells were fused. After cell sorting and/or establishment of myoblast growth, fusion into multinucleated myotubes was induced and muscle cell structure visually confirmed using fluorescent microscopy (Fig. 1). After 4 days of fusion, cells were consistently >75% multinucleated. Muscle cell differentiation with fusion was confirmed by increases in the expression pattern of striated muscle specific sarcomeric α-actin protein as well as CPK-M enzyme activity and mRNA levels (Table 2 and Fig. 2). Cell fusion of myoblasts to myotubes was associated with a 3.5-fold increase in sarcomeric α-actin, a sixfold increase in CPK-M enzyme activity, and a twofold increase in CPK-M mRNA levels (Table 2). Levels of β-actin mRNA, a constitutive or housekeeping protein, were similar in myoblasts and myotubes (Fig. 2).

Insulin and IGF-I receptor binding. Both insulin and IGF-I bound specifically to fused myotubes. Displacement curves for the binding of both hormones (Fig. 3) indicate that more IGF-I was bound than insulin, especially at physiological hormone concentrations. The affinities of each hormone for its own receptor, as well as possible cross-talk between receptors, was investigated by studying displacement of labeled hormone by both the unlabeled ligand and the heterologous hormone. These results are presented in Fig. 4, where values are normalized against specific hormone binding in the absence of unlabeled ligand. An average affinity of the hormone for the receptor was determined by the con-
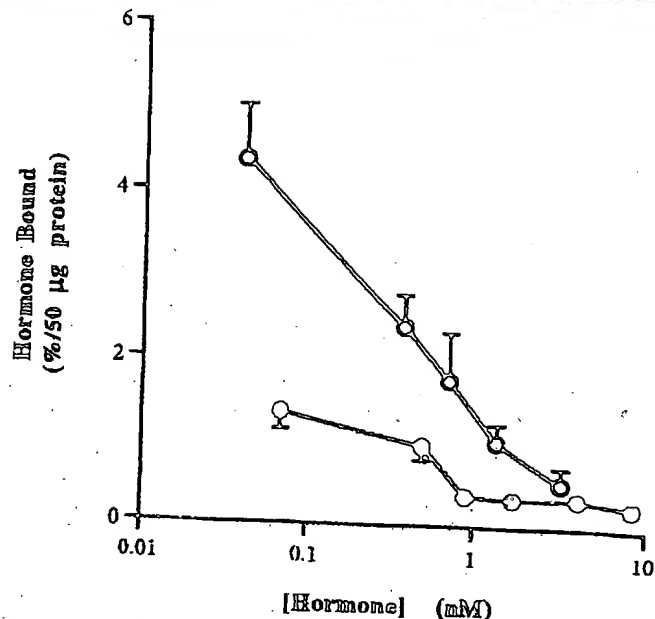

FIG. 3. Insulin (O) and IGF-I (O) receptor binding in fused myotubes as a function of the hormone concentration: percentage of tracer ¹²⁵I-insulin (67 pmol/l) and ¹²⁵I-IGF-I (39 pmol/l) specifically bound per 50 μg total protein. Hormone degradation did not exceed 2% for insulin and 3% for IGF-I. Results are the means ± SE of three to six experiments for each hormone, each performed in triplicate.

centration of unlabeled ligand that displaced 50% of the labeled ligand (EB_{50}). For insulin (Fig. 4A), this value was 0.82 ± 0.08 nmol/l. A high concentration of IGF-I displaced labeled insulin binding by 12–13%. The same insulin concentration inhibited binding by >75%. IGF-I binding to myotubes was also of high affinity (EB_{50} = 0.49 ± 0.09 nmol/l), but insulin was unable to displace labeled IGF-I at physiological concentrations (Fig. 4B).

Glucose transport and disposal. 2-Deoxyglucose uptake in fused myotubes from nondiabetic control subjects was linear for up to 30 min at room temperature in both the absence (basal) and presence of added insulin (33 nmol/l) (not shown). All subsequent experiments were carried out at 15 min to ensure measurement of initial rates of transport. As shown in Table 3, rates of transport increased approximately twofold ($P \leq 0.01$) at 10^{-7} mol/l insulin. Half-maximal stimulation of glucose transport occurred at physiological insulin levels (0.98 ± 0.12 nmol/l) with maximal stimulation at 17.5 nmol/l insulin (Fig. 5). A similar sensitivity was observed to IGF-I. Nonspecific (L-glucose) uptake, due to diffusion, was unaffected at all hormone concentrations (data not shown), indicating that only stereospecific glucose uptake was stimulated by insulin or IGF-I. These results confirm that myotubes have specific carrier-mediated transport that is stimulated by insulin and IGF-I.

The relationship between maximal rates of insulin-stimulated 2-deoxyglucose transport into myotubes was compared with maximal in vivo glucose disposal rates determined by hyperinsulinemic glucose clamps in the same subjects. As shown in Fig. 6, a significant correlation ($r = 0.65$, $P \leq 0.05$) was found to exist between these measures of insulin action in skeletal muscle at both the in vivo and in vitro levels. This correlation included cellular transport and glucose disposal rates from both nondiabetic control and NIDDM subjects.

The presence of the glucose transporter proteins responsible for basal (GLUT1) and insulin-stimulated (GLUT4)
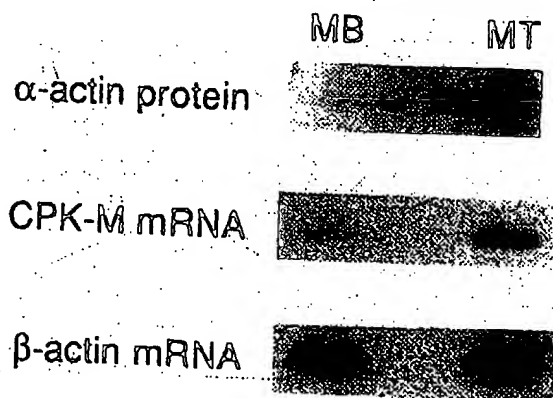

FIG. 2. Western blot analysis of sarcomeric muscle-specific α-actin protein and slot blots of CPK-M and β-actin mRNA in total homogenates of proliferating myoblasts (MB) and differentiated myotubes (MT) from HSMC cultures. Myotubes were fused with a preparation of cellular protein and total RNA was extracted as described under methods. For sarcomeric α-actin 10 μg of total protein were loaded, for CPK-M 10 μg of total RNA and for β-actin 5 μg of total RNA were applied to slot.
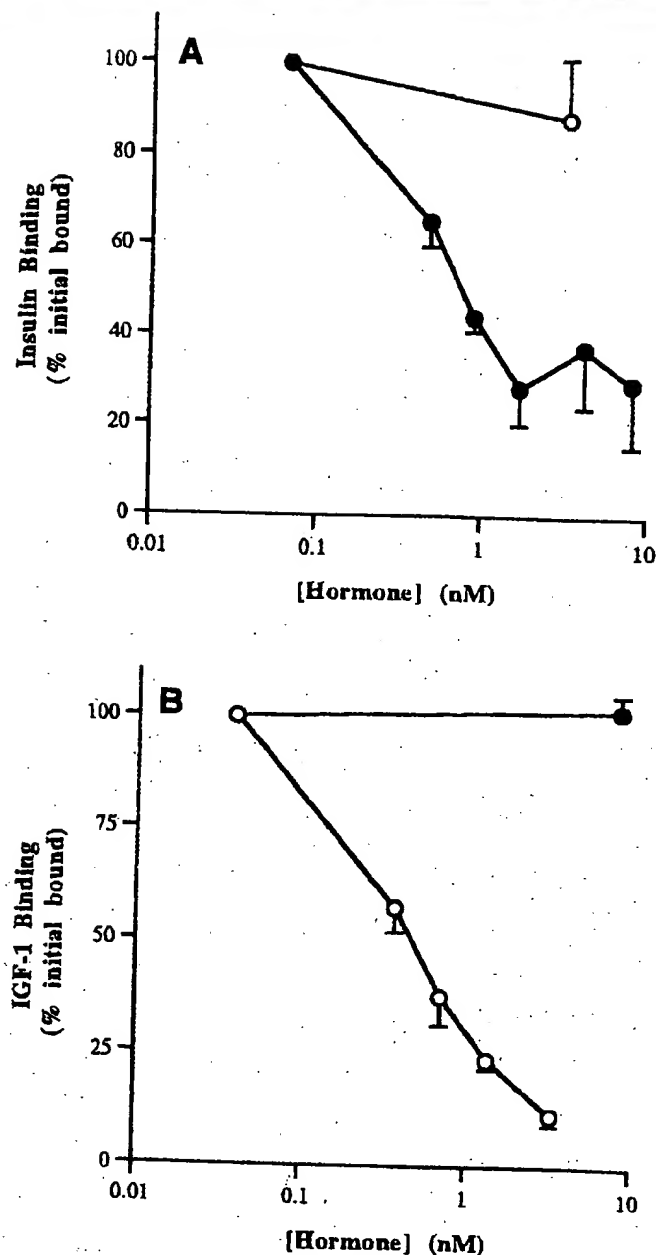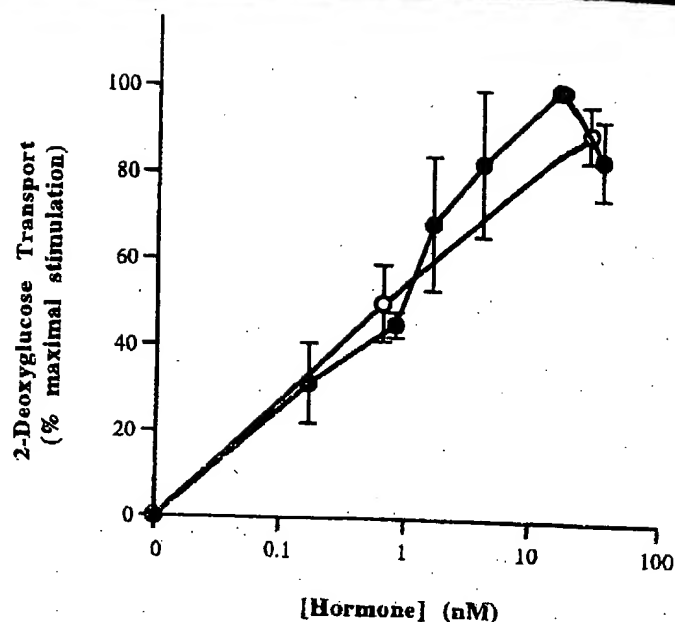
940

FIG. 5. Stimulation of 2-deoxyglucose transport in fused myotubes as a function of insulin (●) and IGF-I (○) concentration. Data are normalized as a function of the maximal hormone effect in each individual culture (*n* = 4), each performed in triplicate, means ± SE.

FIG. 4. Displacement of ¹²⁵I-insulin and ¹²⁵I-IGF-I binding in fused myotubes. *A*: myotubes were incubated with ¹²⁵I-insulin (67 pmol/l) and various amounts of human insulin or IGF-I for 2 h at 24°C. *B*: myotubes were incubated with ¹²⁵I-IGF-I (39 pmol/l) and various concentrations of human IGF-I or insulin for 2 h at 24°C. Results are the means ± SE of four experiments each for insulin (●) and IGF-I (○).

glucose transport and their specific mRNAs were confirmed in fused myotubes of HSMC cultures by Western blot analysis (Fig. 7) and RNase protection assay (Fig. 8), respectively. Affinity-purified GLUT1 and GLUT4 anti-peptide antibodies recognized bands of ~50,000 and 45,000 M_r, respectively. Because of differences in the affinities of the specific antisera for GLUT1 and GLUT4, qualitative conclusions about the relative expression of the two transporters in cultured myotubes cannot be determined from Western blots.

Intracellular enzymes. As shown in Table 3, a 1-h incubation with and without 33 nmol/l insulin demonstrates glucose incorporation into glycogen as well as acute activation of rate-limiting enzymes GS and PDH (29). Glycogen synthesis was stimulated more than double above basal ($P \leq 0.03$) and

was accompanied by a comparable twofold increase in the FV of GS ($P \leq 0.01$). The FV of PDH also increased 30% in response to insulin stimulation ($P \leq 0.05$).

GS and PDH proteins, detected by Western blotting of cell culture homogenates, were present as bands of ~88,000 and 41,000 M_r, respectively (Fig. 7). The mRNAs for GS and PDH in HSMC cultures were present as protected bands of 95 and 80 base pairs, respectively (Fig. 8).

Glucose transport in cells from nondiabetic control and NIDDM subjects. Acute insulin exposure of cells from nondiabetic control subjects resulted in an increase to 203 ± 23% of basal glucose transport activity ($P \leq 0.01$). Cells from NIDDM subjects were also insulin-responsive (increase to 210 ± 23% of basal). However, there were significant differences in glucose transport activity between HSMCs from nondiabetic and NIDDM subjects (Fig. 9). Basal transport activity in cells from NIDDM subjects (6.9 ± 1.0 pmol/mg protein/min) was reduced to 50% of the value in cells from nondiabetic control subjects (13.0 ± 1.7, $P \leq 0.005$). Insulin-stimulated transport activity was also lower in cells from NIDDM subjects (13.5 ± 2.0 vs. 22.4 ± 1.3, $P \leq 0.005$). Thus, HSMCs from NIDDM subjects had a reduced capacity to transport glucose but were still able to respond to insulin, although the absolute magnitude of the response was significantly reduced.

To determine the level of glucose transporter proteins, total membranes were prepared from HSMCs of nondiabetic and NIDDM subjects and analyzed by SDS-PAGE followed by Western blotting with specific antisera. Quantitation of glucose transporter levels in HSMCs from control and NIDDM subjects, determined from scanning densitometry of autoradiograms, is presented in Fig. 10. The expression of GLUT1 in NIDDM cells is reduced to 70% of that in normal cells ($P \leq 0.05$), nearly the same value to which basal transport activity was reduced. GLUT4 protein expression did not differ between the two groups, in contrast with the depressed insulin-stimulated transport activity present in vivo and in vitro (Fig. 9).

TABLE 3
Acute insulin stimulation of glucose transport, glycogen synthesis, GS, and PDH activity in HSMC

	Basal	Stimulated
Glucose transport (17) (pmol · mg protein^{-1} · min^{-1})	13.0 ± 1.7	22.4 ± 1.3†
Glycogen synthesis (10) (nmol glucose · mg protein^{-1} · h^{-1})	0.988 ± 0.204	2,101 ± 0.445‡
GS (13) (nmol · mg protein^{-1} · min^{-1})		
Glucose-6-phosphate, 0.1 mmol/l	0.22 ± 0.02	0.47 ± 0.06†
Glucose-6-phosphate, 10 mmol/l	2.67 ± 0.18	3.09 ± 0.22†
FV (%)	8.15 ± 0.67	16.15 ± 2.11†
Pyruvate dehydrogenase (5) (nmol · mg protein^{-1} · min^{-1})		
PDHa	1.02 ± 0.27	1.24 ± 0.29
PDHt	2.33 ± 0.54	2.23 ± 0.65
FV (%)	43.26 ± 6.89	56.30 ± 4.79§

Data are means ± SE. Basal indicates no added insulin; stimulated indicates 33 nmol/l insulin added for 60–90 min. Numbers of cultures tested are shown in parentheses. PDHa, active PDH; PDHt, total PDH; FV, fractional velocity defined as percentage of activity at 0.1/10 mmol/l glucose-6-phosphate for GS and PDHa/PDHt for PDH. †$P \leq 0.01$; ‡$P \leq 0.03$; §$P \leq 0.05$.

DISCUSSION

Despite the importance of skeletal muscle in insulin-mediated glucose disposal, including a crucial role as a site of insulin resistance in obesity and NIDDM, the current means for studying muscle metabolism have numerous limitations. The HSMC culture technique was modified and characterized as an in vitro system to permit studies of insulin action and cellular glucose metabolism to be performed in adult human skeletal muscle tissue under standardized experimental conditions. There are a number of advantages of this HSMC culture system that require emphasis. First, cultures can be readily established from as little as 250 mg of muscle tissue, an amount that is easily accessible from needle biopsy with minimal invasiveness. Second, large numbers of well-characterized subjects can be studied with this technique. An additional advantage is that repeat biopsies can be obtained from the same subject to study the effects of in vivo manipulation on insulin action and glucose metabolism. Moreover, this system permits evaluation of insulin action in

metabolically relevant tissue without confounding hormone or substrate variables usually present in vivo while still allowing for the detailed, independent manipulation of such variables.

The methodology for growth and maintenance of adult human skeletal muscle has recently been developed and utilized in several laboratories (4,5,8,9,30), but the widespread application of these techniques had been limited by difficulty with tissue availability. It has previously been suggested that needle biopsy specimens could be adapted as a suitable source of muscle cultures (4). The current study not only confirms this impression but expands the potential of the technique as an accurate model to compare and study subjects with NIDDM as well.

For HSMC cultures to be accepted as an accurate model to investigate insulin action in human skeletal muscle tissue, it must be demonstrated that HSMCs are both muscle cells and are reflective of the metabolic behavior of skeletal muscle. To do so, several features of the system need to be clearly defined. It is imperative that the cultures consist solely of muscle cells, and this was confirmed by fluorescence-activated cell sorting. Visual evidence of muscle cell differentiation was provided by fluorescence microscopy demonstrating cell fusion, multinucleation, and the presence of striations using skeletal muscle–specific myosin-fast stains. Induction of muscle-specific proteins during differentiation was confirmed by Western blots, which demonstrated increased sarcomeric muscle-specific α-actin and slot blots of increased CPK-M mass as well as increased CPK enzyme activity after fusion. The proteins responsible for basal (GLUT1) and insulin-stimulated (GLUT4) glucose transport and the rate-limiting enzymes for glucose oxidation (PDH) and glycogen synthesis (GS) were also identified by Western blotting, as were their respective mRNAs by an RNase protection assay. Since expression of the GLUT4 protein is specific only for fully differentiated adipocytes and striated muscle (16), the presence of GLUT4 in HSMCs could be interpreted as an additional marker of the differentiated status of the cells. As well as these morphological and biochemical markers, myotubes were shown to resemble muscle tissue metabolically, with intact insulin and IGF-1 receptor signaling cascades that led to stimulation of glucose transport and activation of PDH and GS activity with increased glycogen formation.

The presence of GLUT1 in muscle has been a matter of debate in the literature. Earlier studies identified the majority
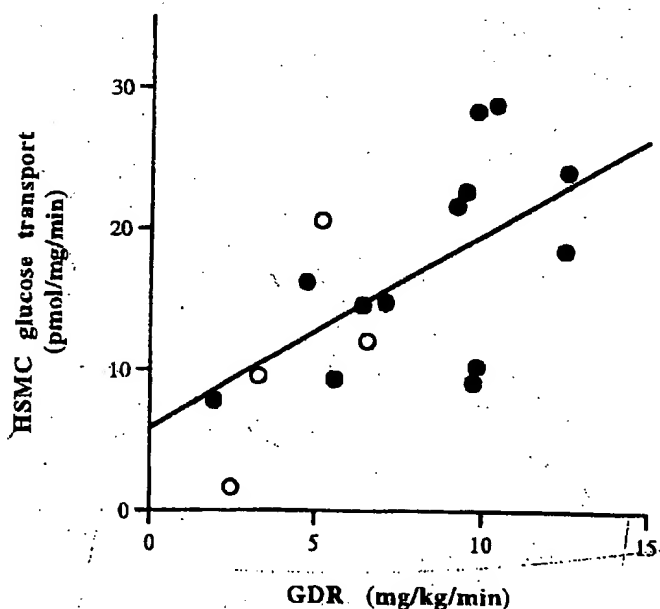

FIG. 6. Relationship between in vivo glucose disposal rate (GDR) during hyperinsulinemic (720 pmol · m^{-2} · min^{-1}) euglycemic clamp and insulin-stimulated 2-deoxyglucose transport in HSMCs from 13 lean and obese control subjects with normal glucose tolerance (●) and 4 subjects with NIDDM (○). Rates of glucose disposal and 2-deoxyglucose transport were determined under maximal insulin-stimulated conditions as described under METHODS ($r = 0.65$, $P \leq 0.05$).
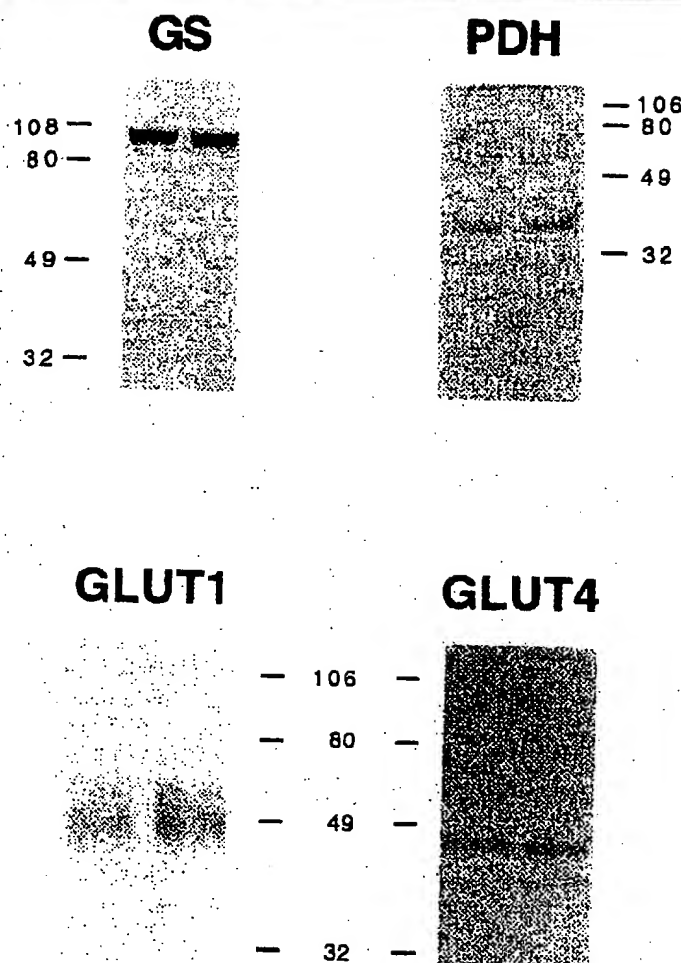
GS

108 —
80 —

49 —

32 —

PDH

— 106
— 80

— 49

— 32

GLUT1

GLUT4

— 106 —

— 80 —

— 49 —

— 32 —

FIG. 7. Expression of GLUT1, GLUT4, GS, and PDH Ela proteins in fused myotubes of HSMC cultures detected using polyclonal antibodies specific for each protein. Samples from multiple cultures were prepared as described under METHODS. For GLUT1 and GLUT4, 25 μg of membrane protein was loaded in each well; for GS, 20 μg of total cellular protein and for PDH, 50 μg were loaded. Locations of molecular weight markers are shown for each blot.

of GLUT1 protein in perineural sheaths of skeletal muscle with little in muscle cells themselves, although that distribution may be muscle type–specific (31). More recent studies, using immunohistochemical techniques, have identified GLUT1 in muscle cells and membranes (31,32). Since our data establish that HSMCs contain a single type of cell, it would appear to eliminate the possible contribution of other cell types to the GLUT1 observed in HSMCs, supporting these later studies. GLUT1 expression is also increased as a cell loses its differentiated phenotype (9). This could also contribute to the presence of GLUT1 in HSMCs, but the numerous markers evaluated in these cultures support the differentiated status of HSMCs and argue against significant dedifferentiation.

The current studies indicate that human myotubes contain specific high-affinity receptors for both insulin and IGF-I that are present in the same relative proportion as in human skeletal muscle (30,33). In addition to the presence of these receptors in skeletal muscle cultures, comparable stimulation of glucose transport in a dose-responsive manner (Fig. 5) by the respective ligand confirms that these receptors exhibit similar sensitivity to both hormones and are coupled to an appropriate metabolic response. The fact that the IGF-I

receptor complement in myotubes exceeds that for insulin might imply that insulin is capable of acting to some extent through the IGF-I receptor. However, insulin had no discernible effect in displacing IGF-I binding at physiological insulin concentrations. Therefore, it seems unlikely that insulin leads to significant stimulation of glucose transport by cross-talk with the IGF-I receptor but acts primarily through its own receptor. The high sensitivity of glucose transport to IGF-I is consistent with IGF-I stimulation through its own receptor as well. The insulin sensitivity of glucose transport stimulation in HSMCs ($EC_{50} \simeq 1$ nmol/l) is 30-fold greater than that in the murine L6 myoblasts (16) and is probably more reflective of the physiological situation in humans. Increased insulin sensitivity may be a species-specific property since Sarabia et al. (4,16) have also reported EC_{50} values for transport stimulation in cultured human muscle cells, similar to those found in the current report, that are an order of magnitude less and therefore more sensitive than L6 cells.

The maximal stimulation of glucose transport in HSMC myotubes (twofold) is somewhat less than is commonly observed for insulin stimulation of in vivo glucose uptake into skeletal muscle (1,2). This discrepancy between in vivo and in vitro insulin stimulation of muscle glucose uptake raises some concern about how reflective the HSMC system may be of intact skeletal muscle. While comparable degrees of stimulation might be expected to occur in the two systems, a number of studies indicate that the relative responsiveness of glucose transport to insulin determined in vivo (34), in isolated human skeletal muscle preparations

Probes | Protected Fragments

| | | GS | PDH | Glut1 | Glut4 |

GS PDH Glut1 Glut4   — + +   — + +   — +   — +
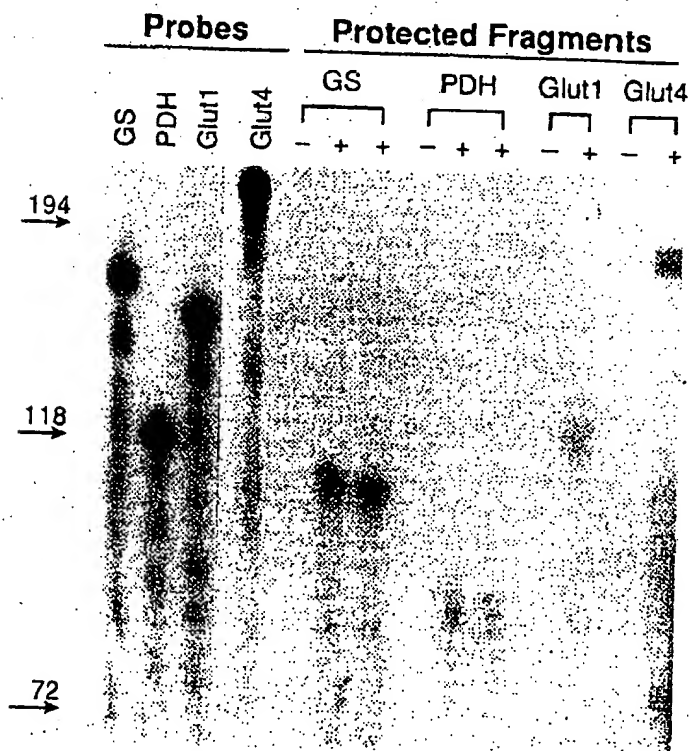
194 →

118 →

72 →

FIG. 8. Autoradiograph of GLUT1, GLUT4, GS, and PDH Ela mRNA abundance determined by RNase protection assay from fused myotubes of HSMC cultures. Samples were prepared as described under METHODS. For GLUT1, 50 μg of total RNA was loaded, for GLUT4, 115 μg, and for GS and PDH, 25 μg each. Negative control lanes of probe plus 10 μg yeast tRNA were included with each protected fragment and are shown by –. Lanes for GS, PDH, and GLUT1 were exposed to film for 24 h and lanes for GLUT4 for 96 h. Locations of molecular weight markers are shown on the left.
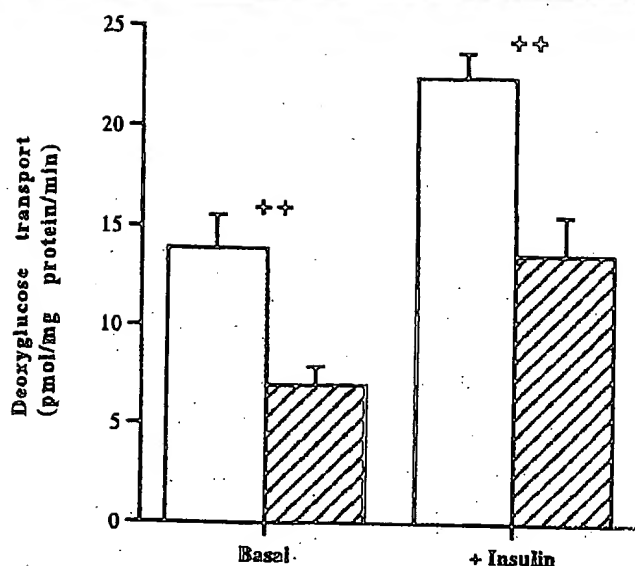
FIG. 9. Comparison of glucose transport activity in HSMCs from nondiabetic control and NIDDM subjects. Cells were grown in low insulin (22 pmol/l) and fused as described under METHODS. Cells were washed and incubated in serum-free α-MEM for 60–90 min in the absence (basal) or presence (33 nmol/l) of insulin. Cells were then washed free of media, and 2-deoxyglucose uptake was measured. Each measurement was performed in triplicate, and each value was corrected for trapping and diffusion as well as protein. ▢, nondiabetic control subjects (n = 11); ▨, NIDDM subjects (n = 14). Results are means ± SE; ++P ≤ 0.005.

(35–38), and in plasma membrane vesicles of rat skeletal muscle (39,40) is not comparable to that reported for in vivo glucose uptake.

Bonadonna et al. (34) have reported on a technique to measure whole body and forearm glucose utilization as well as glucose transport into skeletal muscle. While they found an approximately sevenfold increase in forearm glucose uptake in normal control subjects during hyperinsulinemia, fractional glucose transport into forearm muscle, using 3-O-methylglucose, only doubled in response to insulin. With in vitro preparations (35–38), the typical maximal effect of insulin on glucose transport was reported as a two- to threefold stimulation. Thus, it would appear that the average capacity of skeletal muscle glucose transport to respond to insulin as measured in all of these various muscle preparations does not correspond to the augmentation that normally occurs for in vivo insulin-stimulated glucose uptake. This would suggest that other factors, such as blood flow, non-cellular glucose compartments, circulating factors, and other nonmuscle tissues, may make a considerable contribution to the insulin responsiveness of glucose uptake measured in vivo. A major advantage of the HSMC system is that these confounding variables either do not exist or can be readily controlled or accounted for. In comparison with glucose transport results in the current report, other investigators who have evaluated glucose transport into cultured human muscle cells have found an average insulin stimulation of 35–60% (4,9). Thus, the methodology and modifications that we have applied to the culture and differentiation conditions appear to have improved the responsiveness of the glucose transport system to a degree comparable with other in vitro systems.

Although a one-to-one relationship does not exist between the magnitude of insulin stimulation of in vivo glucose uptake and glucose transport measured in our system or that of others, a significant correlation was found in the current

study when maximal insulin-stimulated rates of 2-deoxyglucose transport in HSMC cultures of individuals were compared with their glucose disposal rates determined during hyperinsulinemic clamps (Fig. 6). That is, a positive relationship was present between in vivo and in vitro measures of glucose uptake such that individuals with a low maximal rate of insulin-stimulated glucose disposal tended to have low maximal rates of insulin-stimulated glucose transport in their HSMC cultures.

Having satisfied ourselves that HSMCs are sufficiently similar to skeletal muscle to serve as an accurate model system, we set out to use the advantages of a cell system—full exposure of cells to media, technical ease for assay of initial rates of transport, and independent manipulation of variables—to study glucose transport regulation. The data in Fig. 9 reveal that HSMCs from NIDDM subjects display decreased glucose transport activity. The transport defect in HSMCs was reflective of differences in peripheral glucose disposal measured in vivo (34,41–43), a further advantage of this system. The average 50% reduction in maximally insulin-stimulated glucose transport in cells from NIDDM subjects compared with those from nondiabetic control subjects is of the same magnitude as that seen for peripheral glucose uptake in these and other subjects (7,41–43), forearm transmembrane glucose transport measured in vivo (34) or with isolated muscle strips in vitro (35,36), and in isolated adipocytes (44–47). These results provide further evidence that the metabolic behavior of HSMCs resembles events in skeletal muscle tissue.

The retention of this glucose transport defect, even after extended time in culture, suggests that impaired glucose transport in NIDDM subjects is the result of either a genetic or a nonreversible acquired defect and is not necessarily a result of the hormonal and metabolic milieu. While the HSMC system is not strictly a primary culture system, culture for multiple passages would be required to firmly establish a
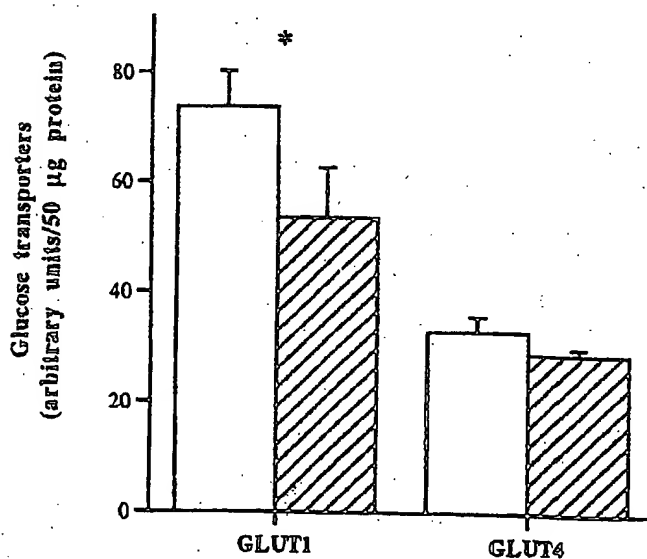

FIG. 10. Comparison of glucose transporter isoform expression in HSMCs from nondiabetic control and NIDDM subjects. Cells were grown in 22 pmol/l insulin as described in the legend to Fig. 1. Total membranes were prepared, proteins were separated on SDS-PAGE, and Western blot analysis was performed as described under METHODS. Quantitation of GLUT1 and GLUT4 was performed by scanning densitometry of HSMCs from nondiabetic control (▢, n = 7) and NIDDM (▨, n = 8) subjects. Results are means ± SE and are normalized to the amount of membrane protein loaded on the gel. *P ≤ 0.05.

genetic basis for the transport defect. Impaired insulin-stimulated glucose transport activity in the presence of normal total GLUT4 content (compare Figs. 9 and 10) is a finding that is also in agreement with numerous in vivo studies (48–51), providing additional evidence that findings in HSMCs and skeletal muscle tissue are concordant. Since GLUT4 expression was measured in total membranes, no conclusions can be drawn about changes in subcellular distribution of transporters or impaired translocation in response to insulin as possible causes of decreased insulin-stimulated transport in NIDDM.

We also considered the possibility that the abnormalities present in cultures from NIDDM subjects might be an indication of the growth characteristics of diabetic tissue rather than an accurate representation of insulin resistance. That is, due to the multiple metabolic abnormalities that exist in muscle of NIDDM subjects, it might grow less well in culture, which would result in a reduced level of metabolic machinery including glucose transport. Several aspects of our results lead us to believe that this is not a likely explanation. If this were the case, we would expect GLUT4 levels to also be reduced as we found for GLUT1. It would also be unlikely for a relationship to exist between glucose transport measured in vitro and in vivo glucose uptake activity. Although these findings are not confirmatory, they support that this culture system does provide an index of insulin resistance in muscle tissue of both nondiabetic and NIDDM subjects.

In summary, a technique has been adapted to allow human skeletal muscle to be grown in culture with ease and simplicity. After myoblast growth and fusion into multinucleated myotubes, these cells manifest numerous morphological, biochemical, and metabolic characteristics of differentiated skeletal muscle and demonstrate many of the components necessary for an accurate evaluation of insulin action and glucose metabolism in muscle tissue. HSMC cultures display dynamic responsiveness to insulin stimulation that is similar to events occurring in muscle tissue in vivo. The in vitro behavior of this muscle culture system may provide a unique opportunity to study glucose metabolism and insulin action in normal and disease states of humans.

REFERENCES

1. DeFronzo RA, Jacot E, Jequier E, Maeder E, Wahren J, Felber JP: The effect of insulin on the disposal of intravenous glucose: results from indirect calorimetry and hepatic and femoral venous catheterization. *Diabetes* 30:1000–1007, 1981
2. Laakso M, Edelman SV, Olefsky JM, Brechtel G, Wallace P, Baron AD: Kinetics of in vivo muscle insulin-mediated glucose uptake in human obesity. *Diabetes* 39:965–974, 1990
3. DeFronzo RA, Bonadonna RC, Ferrannini E: Pathogenesis of NIDDM: a balanced overview. *Diabetes Care* 15:318–368, 1992
4. Sarabia V, Lam L, Burdett E, Leiter LA, Klip A: Glucose transport in human muscle cells in culture: stimulation by insulin and metformin. *J Clin Invest* 90:1386–1395, 1992
5. Klip A, Tsakiridis T, Marette A, Ortiz PA: Regulation of expression of glucose transporters by glucose: a review of studies in vivo and in cell cultures. *FASEB J* 8:43–53, 1994
6. National Diabetes Data Group: Classification and diagnosis of diabetes mellitus and other categories of glucose intolerance. *Diabetes* 28:1039–1057, 1979
7. Thorburn AW, Gumbiner B, Bulacan F, Wallace P, Henry RR: Intracellular glucose oxidation and glycogen synthase activity are reduced in non-insulin dependent (type II) diabetes independent of impaired glucose uptake. *J Clin Invest* 85:522–529, 1990
8. Blau HM, Webster C: Isolation and characterization of human muscle cells. *Proc Natl Acad Sci USA* 78:L5623–L5027, 1981
9. Sarabia V, Lam L, Burdett E, Leiter LA, Klip A: Glucose uptake in human and animal muscle cells in culture. *Biochem Cell Biol* 68:536–542, 1990
10. Webster C, Pavlath GK, Parks DR, Walsh FS, Blau HM: Isolation of human myoblasts with a fluorescence-activated cell sorter. *Exp Cell Res* 17:262–265, 1988
11. Feramisco JR: Microinjection of fluorescently labeled α-actinin into living fibroblasts. *Proc Natl Acad Sci USA* 76:3967–3971, 1979
12. Lalande ME, Ling V, Miller RG: Hoechst 33342 dye uptake as a probe of membrane permeability changes in mammalian cells. *Proc Natl Acad Sci USA* 78:363–367, 1981
13. van der Ven PFM, Schaart G, Jap PHK, Sengers RCA, Stahhouders AM, Ramaekers FCS: Differentiation of human skeletal muscle cells in culture: maturation as indicated by titan and desmin striation. *Cell Tissue Res* 270:189–198, 1992
14. Ciaraldi TP, Gilmore A, Olefsky JM, Goldberg M, Heidenreich KA: In vitro studies on the action of CS-045, a new antidiabetic agent. *Metabolism* 39:1056–1062, 1990
15. Klip A, Li G, Logan WJ: Induction of sugar uptake response to insulin by serum depletion in fusing L6 myoblasts. *Am J Physiol* 247:E291–E296, 1984
16. Sarabia V, Ramlal T, Klip A: Glucose uptake in human and animal muscle cells in culture. *Biochem Cell Biol* 68:536–542, 1990
17. Bradford MM: A rapid and sensitive method for the quantitation of microgram quantities of protein utilizing the principle of protein-dye binding. *Anal Biochem* 71:248–254, 1976
18. Thorburn AW, Gumbiner B, Bulacan F, Brechtel G, Henry RR: Multiple defects of muscle glycogen synthase activity contribute to reduced glycogen synthesis in non-insulin dependent diabetes mellitus. *J Clin Invest* 87:489–495, 1991
19. Suh K-I, Murata C, Song Y-M, Joyce M, Gumbiner B, Ditzler TM, Henry RR: Intracellular glucose metabolism after long-term metabolic control with glyburide: improved glucose oxidation with unchanged glycogen synthase activity. *J Clin Endocrinol Metab* 77:464–470, 1993
20. Ciaraldi TP, Goldberg M, Odom R, Stolpe M: In vitro effects of Amylin on carbohydrate metabolism in liver cells. *Diabetes* 41:975–981, 1992
21. Browner MF, Nakano K, Bang AG, Fletterick RF: Human muscle glycogen synthase cDNA sequence: a negatively charged protein with an asymmetric charge distribution. *Proc Natl Acad Sci USA* 86:1443–1447, 1989
22. Ho L, Wexler ID, Liu T-C, Thekkumkara TJ, Patel MS: Characterization of cDNAs encoding human pyruvate dehydrogenase E1α-subunit. *Proc Natl Acad Sci USA* 86:5330–5334, 1989
23. Goodman EM, MacDonald RJ: Cloning of hormone genes from a mixture of cDNA molecules. *Methods Enzymol* 68:75–90, 1990
24. Saiki RK, Gelfand DH, Stoffel S, Scharf SJ, Higuchi R, Horn GT, Mullis KB, Erlich HA: Primer-directed enzymatic amplification of DNA with a thermostable DNA polymerase. *Science* 239:487–491, 1988
25. Tabor S, Richardson CC: DNA sequence analysis with a modified bacteriophage T7 DNA polymerase. *Proc Natl Acad Sci USA* 84:4767–4771, 1987
26. Walker PS, Ramlal T, Sarabia V, Koivisto U-M, Bilan PJ, Pessin JE, Klip A: Glucose transport activity in L6 muscle cells is regulated by the coordinate control of subcellular glucose transporter distribution, biosynthesis, and mRNA transcription. *J Biol Chem* 265:1516–1523, 1990
27. Laemmli UK: Cleavage of structural proteins during the assembly of the head of bacteriophage T4. *Nature* 22:680–686, 1970
28. Towbin H, Staehelin T, Gordon J: Electrophoretic transfer of proteins from polyacrylamide gels to nitrocellulose sheets: procedure and some applications. *Proc Natl Acad Sci USA* 76:4360–4354, 1979
29. Mandarino LJ, Wright KS, Verity LS, Nichols J, Bell JM, Kolterman OG, Beck-Nielsen H: Effects of insulin infusion on human skeletal muscle pyruvate dehydrogenase, phosphofructokinase, and glycogen synthase. *J Clin Invest* 80:655–663, 1987
30. Shimizu M, Webster C, Morgan DO, Blau HM, Roth RA: Insulin and insulinlike growth factor receptors and responses in cultured human muscle cells. *Am J Physiol* 251:E611–E615, 1986
31. Doria-Medina CL, Lund DD, Pasley A, Sandra A, Sivitz WI: Immunolocalization of GLUT-1 glucose transporter in rat skeletal muscle and in normal and hypoxic cardiac tissue. *Am J Physiol* 265:E454–E464, 1993
32. Handberg A, Kayser L, Hoyer PE, Micheelsen J, Vinten J: Elevated GLUT1 level in crude muscle membranes from diabetic Zucker rats despite a

normal GLUT1 level in perineural sheaths. *Diabetologia* 37:443–448, 1994

33. Livingston N, Pollare T, Lithell H, Arner P: Characterization of insulin-like growth factor I receptor in skeletal muscle of normal and insulin resistant subjects. *Diabetologia* 31:871–877, 1988

34. Bonadonna RC, Del Prato S, Saccomani MP, Bonora E, Gulli G, Ferrannini E, Bier D, Cobelli C, DeFronzo RA: Transmembrane glucose transport in skeletal muscle of patients with non-insulin-dependent diabetes. *J Clin Invest* 92:486–494, 1993

35. Andreasson K, Galuska D, Thorne A, Sonnenfeld T, Wallberg-Hendriksson H: Decreased insulin-stimulated 3-0-methylglucose transport in in vitro incubated muscle strips from type II diabetic subjects. *Acta Physiol Scand* 142:255–260, 1991

36. Dohm GL, Tapscott EB, Pories WJ, Dabbs DJ, Flickinger EG, Meelheim D, Fushiki T, Atkinson SM, Elton CW, Caro JF: An in vitro human muscle preparation suitable for metabolic studies: decreased insulin stimulation of glucose transport in muscle from morbidly obese and diabetic subjects. *J Clin Invest* 82:486–494, 1988

37. Zierath JR, Galuska D, Nolte LA, Thorne A, Smedegaard Kristensen J, Wallberg-Hendriksson H: Effects of glycaemia on glucose transport in isolated skeletal muscle from patients with NIDDM: in vitro reversal of muscular insulin resistance. *Diabetologia* 37:270–277, 1994

38. Elton CW, Tapscott EB, Pories WJ, Dohm GL: Effect of moderate obesity on glucose transport in human muscle. *Horm Metab Res* 26:181–183, 1994

39. Goodyear LJ, Hirshman MF, Valyou PM, Horton ES: Glucose transporter number, function, and subcellular distribution in rat skeletal muscle after exercise training. *Diabetes* 41:1091–1099, 1992

40. Sternlicht E, Barnard RJ, Grimditch GK: Mechanism of insulin action on glucose transport in rat skeletal muscle. *Am J Physiol* 254:E633–E638, 1988

41. Butler PC, Kryshak EJ, Marsh M, Rizza RA: Effect of insulin on oxidation of intracellularly and extracellularly derived glucose in patients with NIDDM: evidence for primary defect in glucose transport and/or phosphorylation but not oxidation. *Diabetes* 39:1373–1380, 1990

42. DeFronzo RA, Gunnarsson R, Bjorkman O, Olsson M, Wahren J: Effects of insulin on peripheral and splanchnic glucose metabolism in non-insulin-dependent (type II) diabetes mellitus. *J Clin Invest* 76:149–155, 1985

43. Baron AD, Laakso M, Brechtel G, Edelman SV: Reduced capacity and affinity of skeletal muscle for insulin-mediated glucose uptake in noninsulin-dependent diabetic subjects. *J Clin Invest* 87:1186–1194, 1991

44. Ciaraldi TP, Kolterman OG, Scarlett JA, Kao M, Olefsky JM: Role of glucose transport in the post-receptor defect of non-insulin dependent diabetes mellitus. *Diabetes* 31:1016–1022, 1982

45. Kashiwagi A, Verso MA, Andrews J, Vasquez B, Reaven G, Foley JE: In vivo insulin resistance of human adipocytes isolated from subjects with non-insulin-dependent diabetes mellitus. *J Clin Invest* 72:1246–1254, 1983

46. Sinha MK, Raineri-Maldonado C, Buchanan C, Pories WJ, Carter-Su C, Pilch PF, Caro JF: Adipose tissue glucose transporters in NIDDM: decreased levels of muscle/fat isoform. *Diabetes* 40:472–477, 1991

47. Garvey WT, Maianu L, Huecksteadt TP, Birnbaum MJ, Molina JM, Ciaraldi TP: Pretranslational suppression of a glucose transporter protein correlates with cellular insulin resistance in non-insulin-dependent diabetes mellitus and obesity. *J Clin Invest* 87:1072–1081, 1991

48. Pedersen O, Bak JF, Andersen PH, Lund S, Moller DE, Flier JS, Kahn BB: Evidence against altered expression of GLUT1 or GLUT4 in skeletal muscle of patients with obesity or NIDDM. *Diabetes* 39:865–870, 1990

49. Handberg A, Vaag A, Damsbo P, Beck-Nielsen H, Vinten J: Expression of insulin regulatable glucose transporters in skeletal muscle from type 2 (non-insulin-dependent) diabetic patients. *Diabetologia* 33:625–627, 1990

50. Eriksson J, Koranyi L, Bourey R, Schalin-Jantti C, Widen E, Mueckler M, Permutt AM, Groop LC: Insulin resistance in type 2 (non-insulin-dependent) diabetic patients and their relatives is not associated with a defect in the expression of the insulin-responsive glucose transporter (GLUT-4) gene in human skeletal muscle. *Diabetologia* 35:143–147, 1992

51. Garvey WT, Maianu L, Hancock JA, Golichowski AM, Baron A: Gene expression of GLUT4 in skeletal muscle from insulin resistant patients with obesity, IGT, GDM, and NIDDM. *Diabetes* 41:465–475, 1992
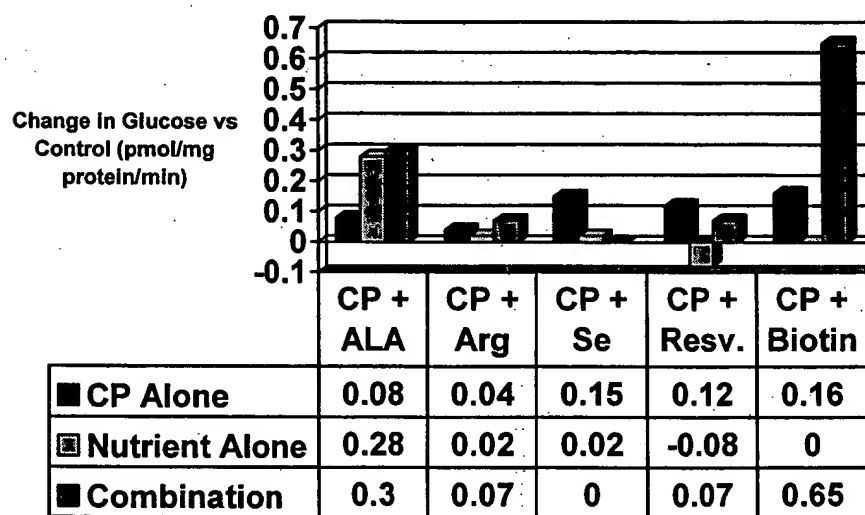
Table 2: 2-Deoxyglucose Values

Nutrient	Concentration*	Glucose Uptake		
		Basal	Insulin-Stimulated	% Change
Chromium Picolinate (CrPic)	0	1.16 ± 0.10	1.56 ± 0.12	34.5
	2	1.15 ± 0.04	1.63 ± 0.20	41.7
	4	1.13 ± 0.03	1.64 ± 0.08	45.1
	8	1.17 ± 0.07	1.70 ± 0.13	45.3
	10	1.14 ± 0.09	1.78 ± 0.06	56.1
	20	1.10 ± 0.03	1.88 ± 0.04	71.0
α-lipoic Acid (αLA)	Control	1.17 ± 0.07	1.57 ± 0.09	34.2
	30	1.14 ± 0.03	1.68 ± 0.16	47.4
	300	1.20 ± 0.05	1.85 ± 0.20	54.2
	CrPic 5/αLA 30	1.07 ± 0.02	1.69 ± 0.07	57.9
	CrPic 5/αLA 300	1.10 ± 0.07	1.78 ± 0.09	61.8
	CrPic 20/αLA 30	1.11 ± 0.04	1.65 ± 0.07	49.5
	CrPic 20/αLA 300	1.20 ± 0.04	1.87 ± 0.02	55.8
	CrPic 5	1.12 ± 0.05	1.62 ± 0.05	44.6
	CrPic 20	1.11 ± 0.01	1.65 ± 0.04	48.6
Picolinic Acid (PA)	0	1.25 ± 0.07	1.46 ± 0.05	16.8
	42.5	1.18 ± 0.08	1.32 ± 0.03	11.9
	85	1.20 ± 0.10	1.37 ± 0.06	14.2
	CrPic 5/PA 85	1.17 ± 0.26	1.44 ± 0.10	23.1
	CrPic 10/PA 85	1.24 ± 0.13	1.52 ± 0.13	22.6
	CrPic 5	1.19 ± 0.18	1.66 ± 0.14	39.5
	CrPic 10	1.22 ± 0.16	1.80 ± 0.07	47.5
Arginine (A)	0	1.46 ± 0.11	1.78 ± 0.04	21.9
	50	1.50 ± 0.06	1.82 ± 0.06	21.3
	500	1.55 ± 0.12	1.80 ± 0.10	16.1
	CrPic 2.5/A 50	1.48 ± 0.11	1.87 ± 0.08	26.4
	CrPic 2.5/A 500	1.42 ± 0.07	1.85 ± 0.07	30.3
	CrPic 2.5	1.40 ± 0.10	1.82 ± 0.10	30.0
Biotin (B)	Control	1.10 ± 0.10	1.52 ± 0.10	38.2
	10	1.07 ± 0.02	1.52 ± 0.06	42.0
	50	1.24 ± 0.09	1.52 ± 0.06	22.6
	CrPic 5/B 10	1.18 ± 0.10	1.76 ± 0.07	49.1
	CrPic10/B 10	1.16 ± 0.01	1.81 ± 0.14	56.0
	CrPic 5/B 50	1.22 ± 0.04	1.97 ± 0.07	61.5
	CrPic 10/B 50	1.26 ± 0.08	2.17 ± 0.20	72.2
	CrPic 5	1.19 ± 0.05	1.70 ± 0.14	42.8
	CrPic 10	1.14 ± 0.10	1.68 ± 0.08	47.4

EXHIBIT C

Figure 1.   Glucose Update in Human Skeletal Muscle Cells

	CP + ALA	CP + Arg	CP + Se	CP + Resv.	CP + Biotin
■ CP Alone	0.08	0.04	0.15	0.12	0.16
▨ Nutrient Alone	0.28	0.02	0.02	-0.08	0
■ Combination	0.3	0.07	0	0.07	0.65